

Unexpected Molecular Structure of a Putative Rhenium-Dioxo-Benzocarborporphyrin Complex. Implications for the Highest Transition Metal Valence in a Porphyrin-Type Ligand Environment

Abraham B. Alemayehu,^[a] Hugo Vazquez-Lima,^[b] Simon J. Teat,^[c] and Abhik Ghosh^{*,[a]}

A combination of quantum chemical calculations and synthetic studies was used to address the possibility of very high (>6) valence states of transition metals in porphyrin-type complexes. With corrole as a supporting ligand, DFT calculations ruled out Re(VII) and Ir(VII) dioxo complexes as stable species. Attempted rhenium insertion into benzocarborporphyrin (BCP) ligands on the other hand led to two products with different stoichiometries – Re[BCP]O and Re[BCP]O₂. To our surprise, single-crystal structure determination of one of the complexes of the latter type indicated an Re^{VO} center with a second oxygen bridging the Re–C bond. In other words, although the monooxo complexes Re[BCP]O are oxophilic, the BCP ligand cannot sustain a *trans*-Re^{VII}(O)₂ center. The search for metal valence states >6 in porphyrin-type ligand environments must therefore continue.

Chemists are perennially interested in exploring the limits of chemical structure and bonding. In recent years, many inorganic chemists, for example, have concerned themselves with determining the highest possible valence or oxidation states for different transition metals. Some notable experimentally established examples of unusually high oxidation states include Au(V), Hg(IV), and Ir(IX) in the form of AuF₆⁻,^[1] HgF₄,^[2] and the IrO₄⁺ cation,^[3] respectively.^[4] In our own laboratory, quantum chemical studies have suggested that the seventh-

period compounds CnF₄^[5] and RgF₇^[6] should also be moderately stable. Porphyrins have long been known to stabilize high-valent transition metal centers such as Fe(IV),^[7] Mn(V), Cr(V), Ru(VI), and Os(VI).^[8] More recently, we have shown that corroles^[9] can stabilize Ru^{VI}N^[10] and Os^{VI}N^[11] centers as well as Mo(VI)^[12] and W(VI),^[13] the latter in the form of unique eight-coordinate biscorrole complexes. Herein, we report our first results on whether porphyrin-type ligands can stabilize a valence higher than six, focusing on rhenium. Rhenium is particularly promising because its heptavalent state is not only stable with oxide (especially in the form of perrhenate, ReO₄⁻), but also with a variety of carbon ligands and even with hydride, the latter in the form of the unique homoleptic ReH₉²⁻ anion.^[14]

We began our investigation by undertaking a ZORA scalar-relativistic density functional theoretical (DFT) study (B3LYP-D3/ZORA-STO-TZ2P; ADF)^[23,24] of as yet experimentally unknown Re^{VII}O₂ and Ir^{VII}O₂ corrole derivatives (Scheme 1). In the Re



Scheme 1. Molecular structures of putative Re(VII)- and Ir(VII)-dioxo complexes.

[a] Dr. A. B. Alemayehu, Prof. Dr. A. Ghosh
Department of Chemistry
UiT – The Arctic University of Norway
9037 Tromsø, Norway
E-mail: abhik.ghosh@uit.no

[b] Dr. H. Vazquez-Lima
Centro de Química, Instituto de Ciencias
Universidad Autónoma de Puebla
Edif. IC9, CU, San Manuel
72570 Puebla, Puebla, Mexico

[c] Dr. S. J. Teat
Advanced Light Source
Lawrence Berkeley National Laboratory
Berkeley, CA 94720–8229, USA

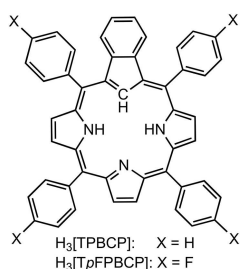
Supporting information for this article is available on the WWW under <https://doi.org/10.1002/open.201900271>

© 2019 The Authors. Published by Wiley-VCH Verlag GmbH & Co. KGaA. This is an open access article under the terms of the Creative Commons Attribution Non-Commercial License, which permits use, distribution and reproduction in any medium, provided the original work is properly cited and is not used for commercial purposes.

case,^[15] the lowest energy structures turned out to be (in order of increasing relative energy) an *S* = 1 *trans*-Re^{VI}(Cor²⁻)(O)₂ species, an *S* = 0 Re^V(η²-O₂) peroxo just 0.12 eV higher in energy, and finally the *S* = 0 *trans* Re^{VII}-dioxo complex 0.39 eV above the ground state. Experimentally as well, attempts to oxygenate Re^{VO} corroles did not yield any indication of an Re^{VII}O₂ product. In the Ir case, we found two essentially equienergetic contenders for the ground state, namely an *S* = 1 *trans*-Ir^{VI}(Cor²⁻)(O)₂ species and the *S* = 0 *trans*-Ir^{VII}(Cor³⁻)(O)₂ species. The Ir^V(η²-O₂) peroxo complex turned out to be some 0.18 eV higher in energy than the lowest-energy Ir-dioxo species. Experimentally, however, the great majority of stable Ir-corroles are six-coordinate Ir(III) complexes^[16] with strongly bound axial amine or phosphine ligands and appear unsuitable as precursors to high-valent Ir-oxo species. One-electron

oxidation of these species also happens in a largely ligand-centered manner, with only a small amount of Ir(IV) character in the final product.^[17]

In the wake of the unpromising exploratory DFT studies on Re and Ir corroles, a significant breakthrough came from an unexpected quarter. While searching for phosphorescent 5d metalloporphyrinoids for use as oxygen sensors and as sensitizers in photodynamic therapy,^[18,19] attempted Re insertion into two different *meso*-tetraarylbenzocarbaporphyrin (BCP)^[20,21] ligands with Re₂(CO)₁₀ in refluxing 1,2,4-trichlorobenzene led to not only Re[BCP]O but also a second product for which high-resolution mass spectrometry indicated a molecular formula "Re[BCP]O₂" (BCP = TPBCP, TpFPBCP; Scheme 2); the



Scheme 2. *Meso*-tetra(*p*-X-phenyl)-substituted benzocarbaporphyrin ligands used in this study.

quotation marks indicate that the formula refers only to stoichiometry but not to connectivity. The key question accordingly was whether the latter contains an Re^{VII}-dioxo center. Both optical and ¹H NMR spectra afforded intriguing clues as to the nature of these two complexes.

All four new Re-benzocarbaporphyrin complexes Re[BCP]O_n (n = 1, 2) were found to exhibit redshifted Soret-like features at just under 500 nm. Interestingly, for both dioxygenated products, the intensity of this feature was found to be only about half that of the monooxo complexes (Figure 1). ¹H NMR spectra also revealed a broader spread of the pyrrole β-protons for the

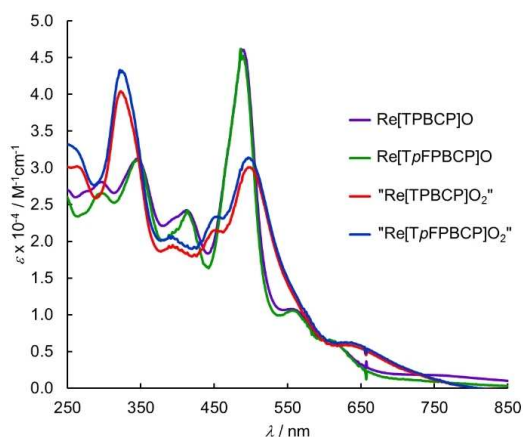


Figure 1. UV/Vis spectra of Re[TPBCP]O, Re[TpFPBCP]O, "Re[TPBCP]O₂" and "Re[TpFPBCP]O₂" in CH₂Cl₂.

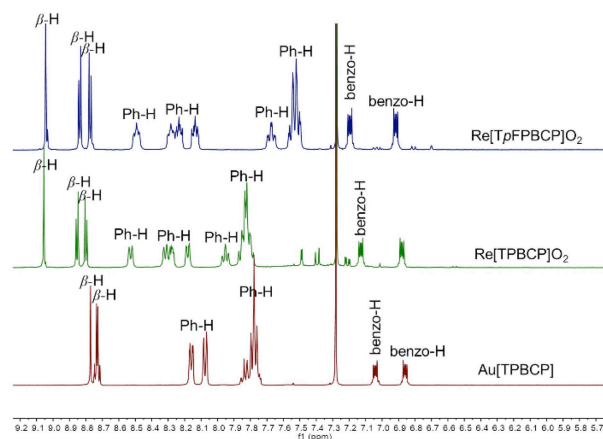


Figure 2. Comparison of the stacked ¹H NMR spectra of "Re[TpFPBCP]O₂" (top), "Re[TPBCP]O₂" (middle) and Au[TPBCP] (bottom) in CDCl₃ at 298 K.

dioxygenated compounds relative to the monooxo complexes (Figure 2). A comparison with the known, structurally characterized, twofold-symmetric gold complex Au[TPBCP] proved instructive.^[20b] Although the *meso*-phenyl protons of the new Re complexes could not be fully assigned because of mutual overlap, it was clear that they led to more numerous signals relative to the Au complex. That is expected for the Re[BCP]O complexes, because of the nonequivalence of the two macrocycle faces, but not for *trans*-Re[BCP]O₂, whose macrocycle faces should be equivalent by symmetry. The ¹H NMR data thus appeared to argue against a *trans*-Re-dioxo formulation.

Fortunately, single-crystal X-ray structures could be obtained for a pair of mono- and dioxygenated complexes, namely Re[TpFPBCP]O and "Re[TpFPBCP]O₂" (Table 1). The former proved much as expected, with equatorial Re–C/N distances of 2.05–2.09 Å and an axial Re–O distance of 1.664(3) Å (Figure 3).

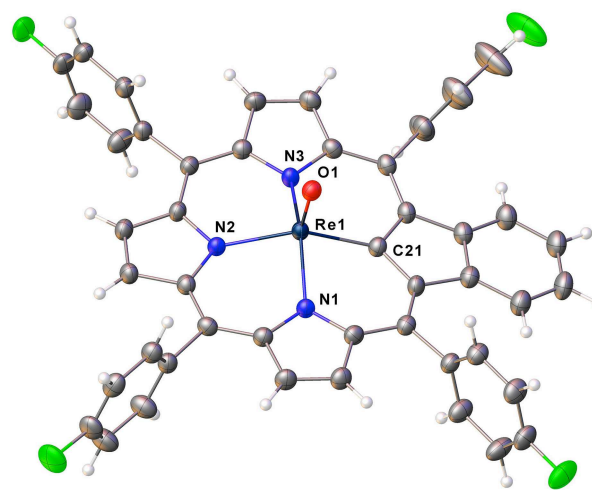


Figure 3. Thermal ellipsoid plot for Re[TpFPBCP]O with probabilities at 50%. Solvent molecules have been omitted for clarity. Selected bond distances (Å): Re1–N1 2.052(3); Re1–N2 2.082(3); Re1–N3 2.058(3); Re1–C21 2.085(4); Re1–O1 1.664(3).

Table 1. Selected crystal and refinement data.

	Re[TpFPBCP]O		"Re[TpFPBCP]O ₂ "	
Empirical formula	C ₄₉ H ₂₆ F ₄ N ₃ ORe		C ₅₀ H ₂₆ Cl ₂ F ₄ N ₃ O ₂ Re	
Formula weight	934.93		1035.85	
Temperature	100(2) K		100(2) K	
Wavelength	0.7288 Å		0.7288 Å	
Crystal system	Monoclinic		Triclinic	
Space group	P2 ₁ /c			
Unit cell dimensions	a = 13.1484(9) Å b = 12.8968(8) Å c = 22.2407(15) Å	α = 90° β = 102.763(3)° γ = 90°.	a = 11.0937(4) Å b = 13.7012(5) Å c = 14.6725(5) Å	α = 87.5400(10)° β = 68.1790(10)° γ = 70.8010(10)°
Volume	3678.2(4) Å ³		1947.22(12) Å ³	
Z	4		2	
Density (calculated)	1.688 Mg/m ³		1.767 Mg/m ³	
Absorption coefficient	3.566 mm ⁻¹		3.521 mm ⁻¹	
F(000)	1840		1020	
Crystal size	0.120 x 0.005 x 0.005 mm ³		0.250 x 0.130 x 0.020 mm ³	
Reflections collected	59818		81871	
Independent reflections	6802 [R(int) = 0.0604]		14856 [R(int) = 0.0317]	
Data / restraints / parameters	6802 / 0 / 528		14856 / 3 / 569	
Goodness-of-fit on F ²	1.035		1.105	
Final R indices [I > 2σ(I)]	R1 = 0.0281, wR2 = 0.0673		R1 = 0.0224, wR2 = 0.0579	
R indices (all data)	R1 = 0.0394, wR2 = 0.0716		R1 = 0.0234, wR2 = 0.0584	

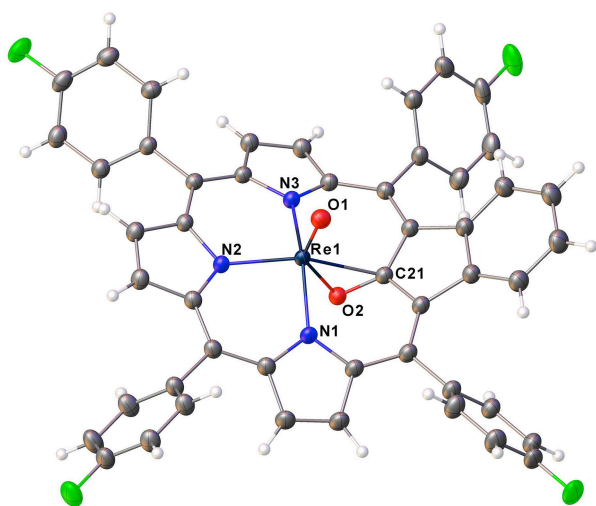
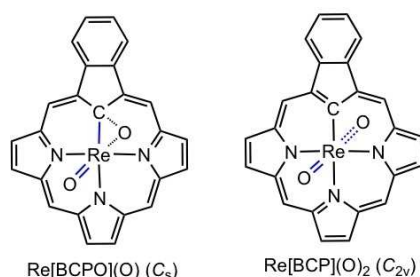


Figure 4. Thermal ellipsoid plot for "Re[TpFPBCP]O₂" with probabilities at 50%. Solvent molecules have been omitted for clarity. Selected bond distances (Å): Re1-N1 2.0823(14); Re1-N2 2.0142(14); Re1-N3 2.0774(14); Re1-C21 2.3017(17); Re1-O1 1.6920(12); Re1-O2 2.0003(12); O2-C21 1.364(2).



Scheme 3. Potential linkage isomers of Re[BCP]O₂.

The structure of "Re[TpFPBCP]O₂", on the other hand, proved unusual. While one of the oxygens (O1) was found to be coordinated as an axial ligand, the other (O2) was found to bridge the Re–C bond, bonded to both atoms as depicted in Figure 4. Comparison of the metal-ligand distances with Pyykkö's additive covalent radii indicated that the Re–O1 distance (~1.69 Å), which is only marginally longer than the Re–O distance in Re[TpFPBCP]O and in ReO corroles,^[15] is consistent with a triple bond, while the Re–O2 distance (~2.00 Å) is consistent with a single bond.^[22] The Re–N and Re–C bond distances are likewise consistent with single bonds. Thus, as shown in Scheme 3, the dioxogenated complexes are best regarded as Re[BCPO](O), where BCPO is a trianionic oxygenated benzocarporphyrin ligand.

Scalar-relativistic DFT (B3LYP-D3/ZORA-STO-TZ2P; ADF) duly indicated the C_s Re[BCPO]O structure as the global minimum, whereas the C_{2v} Re(VII) species *trans*-Re[BCP]O₂, at an energy of 2.1 eV relative to the ground state, was identified as a transition state (Scheme 3). Formally, the BCPO ligand lacks the [18] annulene substructure of porphyrin-type ligands, suggesting reduced aromaticity,^[25] which may explain the low Soret intensity of the dioxogenated complexes, as alluded to above.

DFT calculations and experimental considerations have underscored the difficulties involved in generating Re(VII)- and Ir(VII)-dioxo species with a corrole as the equatorial ligand. Against this backdrop, attempted Re insertion into benzocarporphyrin ligands led to Re[BCP]O_n (n = 1, 2), raising the prospect of an Re^{VII}O₂ complex. A single-crystal X-ray structure, however, indicated a Re^V[BCPO](O) formulation with a ReO triple bond and ReC and ReO single bonds involving the BCPO ligand. DFT calculations confirmed this formulation as the global minimum, while *trans*-Re^{VII}[BCP]O₂ was indicated as a high-energy transition state. The fact that Re^V[BCPO](O) forms at all suggests that the monooxo complex Re^V[BCP]O is oxophilic to a certain degree but that the product cannot sustain a Re(VII) center with BCP as a supporting ligand. Might other equatorial

ligands such as corrolazine stabilize a Re(VII) center? Alternatively, might axial ligands such as imido, nitrido, alkylidene, alkylidyne, and carbido do the trick? These are exciting questions, which we look forward to addressing in the course of ongoing work in our laboratory.

Experimental

Materials. Azulene, 1,2,4-trichlorobenzene, dirhenium decacarbonyl (99.99%), and potassium carbonate (granulated) were purchased from Sigma-Aldrich and used as received. Silica gel 60 (particle size 0.04–0.063 mm, 230–400 mesh, Merck) was employed for flash chromatography. Silica gel 60 preparative thin-layer chromatographic plates (20 cm×20 cm×0.5 mm, Merck) were used for final purification of all complexes.

General instrumental methods. UV-visible spectra were recorded on an HP 8453 spectrophotometer. ¹H NMR spectra (253 K, CD₂Cl₂) were recorded on a 400 MHz Bruker Avance III HD spectrometer equipped with a 5 mm BB/1H SmartProbe and referenced to residual CH₂Cl₂ at 5.31 ppm. High-resolution electrospray-ionization (HR-ESI) mass spectra were recorded on an LTQ Orbitrap XL spectrometer using methanolic solutions and typically in positive ion mode.

Re[TPBCP]O_n (n = 1, 2). To a 50 mL, three-neck, round-bottom flask fitted with a reflux condenser and containing a magnetic stirring bar and 1,2,4-trichlorobenzene (10 mL) was added free-base H₃[TPBCP] (50 mg, 0.0753 mmol), Re₂(CO)₁₀ (98.37 mg, 0.1506 mmol), and potassium carbonate (100 mg). The contents were deoxygenated with a flow of argon and then heated at reflux overnight with constant stirring under Ar. Completion of the reaction was indicated by disappearance of the Soret absorption of the free-base ligand and appearance of a new Soret maximum with λ_{max} ~ 490 nm. Upon cooling, the reaction mixture was directly loaded onto a silica gel column and eluted with n-hexane as the mobile phase, which removed the 1,2,4-trichlorobenzene. Next to elute with 4:1, hexane/dichloromethane was a brown fraction containing monooxo complex Re[TPBCP](O) with a characteristic Soret maximum ~490 nm. A second brown fraction eluted next with 2:1 delete comma here hexane/dichloromethane, containing "Re[TPBCP]O₂" with λ_{max} at 324 and 496 nm. The two distinct fractions were separately collected and further purified by preparative thin-layer chromatography with 4:1 hexane/dichloromethane for the first fraction and 2:1 hexane/dichloromethane for the second fraction.

Re[TPBCP]O. Yield 8 mg (0.0093 mmol, 12.30%). UV/Vis (CH₂Cl₂): λ_{max} (nm; ε × 10⁻⁴, M⁻¹cm⁻¹): 296 (2.80), 343 (3.12), 412 (2.42), 489 (4.60), 554 (1.07). ¹H NMR (400 MHz, 253 K, CD₂Cl₂) δ: 9.12–9.17 (m, 4H, β-H), 9.05–9.06 (s, 2H, β-H), 8.24 (m, 2H, Ph), 8.11 (t, 5H, ³J 7.16 Hz, Ph), 7.76–7.89 (m, 13H, Ph), 7.17–7.19 (dd, 2H, J 5.94 and 3.10 Hz, benzo-H), 6.94–6.97 (dd, 2H, J 5.88 and 3.22 Hz, benzo-H). IR (ATR, diamond): ν_{ReO} 963 cm⁻¹. MS (ESI): m/z calcd for C₄₉H₃₀N₃ORe 864.2022; [M + H]⁺ found 864.2017.

"[Re[TPBCP]O₂." Yield 16 mg (0.0182 mmol, 24.16%). UV/Vis (CH₂Cl₂): λ_{max} (nm; ε × 10⁻⁴, M⁻¹cm⁻¹): 322 (4.04), 452 (2.15), 496 (3.00), 628 (0.59). ¹H NMR (400 MHz, 253 K, CD₂Cl₂) δ: 9.08 (s, 2H, β-H), 8.89 (d, 2H, ³J 4.84 Hz, β-H), 8.84 (d, 2H, ³J 4.88 Hz, β-H), 8.47 (d, 2H, ³J 7.40 Hz, Ph), 7.30 (d, 4H, ³J 7.88 Hz, Ph), 8.16 (d, 2H, ³J 6.36 Hz, Ph), 7.95 (t, 2H, ³J 7.16 Hz, Ph), 7.78–7.87 (m, 10H, Ph), 7.11–7.08 (dd, 2H, J 6.02 and 3.14 Hz, benzo-H), 6.81–6.83 (dd, 2H, J 5.96 and 3.20 Hz, benzo-H). IR (ATR, diamond): ν_{ReO} 966 cm⁻¹. MS (ESI): m/z calcd for C₄₉H₃₀N₃O₂Re: 880.2007 [M + H]⁺; found: 880.1959.

Re[TpFPBCP]O_n (n = 1, 2). The procedure was essentially identical to that described above, except for the quantities of the reactants, which were free-base H₃[TpFPBCP] (60 mg, 0.0816 mmol), Re₂(CO)₁₀ (106.50 mg, 0.1632 mmol), and potassium carbonate (100 mg).

Re[TpFPBCP]O. Yield 10 mg (0.0107 mmol, 13.10%). UV/Vis (CH₂Cl₂): λ_{max} (nm; ε × 10⁻⁴, M⁻¹cm⁻¹): 298 (2.65), 346 (3.10), 413 (2.42), 486 (4.61), 555 (1.05). ¹H NMR (400 MHz, 253 K, CD₂Cl₂) δ: 9.17 (d, 2H, ³J = 4.96 Hz, β-H), 9.14 (d, 2H, ³J = 4.96 Hz, β-H) 9.06 (s, 2H, β-H); 8.28–8.24 (m, 2H, Ph); 8.12–8.05 (m, 6H, Ph); 7.61–7.46 (m, 8H, Ph); 7.26–7.24 (dd, 2H, ³J 5.94 and 2.98 Hz, benzo-H); 7.04–7.01 (dd, 2H, ³J 5.84 and 3.16 Hz, benzo-H);); IR (ATR, diamond): ν_{ReO} 970 cm⁻¹; MS (ESI): m/z calcd for C₄₉H₂₆F₄N₃ORe: 935.1578 [M⁺]; found: 935.1592.

"Re[TpFPBCP]O₂." Yield 18 mg (0.0189 mmol, 23.19%). UV/Vis (CH₂Cl₂): λ_{max} (nm; ε × 10⁻⁴, M⁻¹cm⁻¹): 321(4.33), 454 (2.33), 496 (3.14), 628 (0.62); ¹H NMR (400 MHz, -20 °C, CD₂Cl₂): δ = 9.08 (s, 2H, β-H); 8.88 (d, 2H, ³J(H,H) = 4.84 Hz, β-H); 8.82(d, 2H, ³J(H,H) = 4.92 Hz, β-H); 8.48–8.44 (m, 2H, Ph); 8.30–8.24 (m, 4H, Ph); 8.15–8.12 (m, 2H, Ph); 7.70–7.65 (m, 2H, Ph); 7.57–7.49 (m, 6H, Ph); 7.18–7.15 (dd, 2H, ³J 6.02 and 3.10 Hz, benzo-H); 6.89–6.87 (dd, 2H, ³J 5.92 and 3.20 Hz, benzo-H);); IR (ATR, diamond): ν_{ReO} 970 cm⁻¹; MS (ESI): m/z calcd for C₄₉H₂₆F₄N₃O₂Re: 951.1527 [M⁺]; found: 951.1522.

X-ray quality crystals were obtained by slow diffusion of methanol vapor into concentrated dichloromethane solutions of Re[TpFPBCP]O_n (n = 1, 2).

X-ray crystallography. X-ray data were collected on beamline 12.2.1 at the Advanced Light Source of Lawrence Berkeley National Laboratory, Berkeley, California. The samples were mounted on a MiTeGen® kapton loop and placed in a 100(2) K nitrogen cold stream provided by an Oxford Cryostream 800 Plus low-temperature apparatus on the goniometer head of a Bruker D8 diffractometer equipped with PHOTONII CPAD detector. Diffraction data were collected using synchrotron radiation monochromated with silicon(111) to a wavelength of 0.7288(1) Å. An approximate full-sphere of data was collected using 0.3° ω scans. Absorption corrections were applied using SADABS.^[26] The structure was solved by intrinsic phasing (SHELXT)^[27] and refined by full-matrix least squares on F² (SHELXL-2014).^[28] All non-hydrogen atoms were refined anisotropically. Hydrogen atoms were geometrically calculated and refined as riding atoms.

Acknowledgement

This work was supported by the Research Council of Norway and the Advanced Light Source, Berkeley, California. The Advanced Light Source is supported by the Director, Office of Science, Office of Basic Energy Sciences, of the U.S. Department of Energy under Contract No. DE-AC02-05CH11231.

Conflict of Interest

The authors declare no conflict of interest.

Keywords: corrole · benzocarporphyrin · rhenium · iridium · high-valent compounds

- [1] a) K. Leary, N. Bartlett, *J. Chem. Soc. Chem. Commun.* **1972**, 0, 903; b) K. Leary, A. Zalkin, N. Bartlett, *J. Chem. Soc. Chem. Commun.* **1973**, 0, 131.
- [2] X. Wang, L. Andrews, S. Riedel, M. Kaupp, *Angew. Chem. Int. Ed.* **2007**, 46, 8371.
- [3] a) G. Wang, M. Zhou, J. T. Goettel, G. Schrobilgen, J. Su, J. Li, T. Schlöder, S. Riedel, *Nature* **2014**, 514, 475; b) P. Pyykkö, *Chem. Eur. J.* **2015**, 21, 9468.
- [4] S. X. Hu, W.-L. Li, Lu, J.-B. Bao, H. S. Yu, D. G. Truhlar, J. K. Gibson, J. Marçalo, M. Zhou, S. Riedel, W. H. E. Schwarz, J. Li, *Angew. Chem. Int. Ed.* **2018**, 57, 3242.
- [5] A. Ghosh, J. Conradie, *Eur. J. Inorg. Chem.* **2016**, 2989.
- [6] J. Conradie, A. Ghosh, *Inorg. Chem.* **2019**, 58, 8735.
- [7] For a special issue on diverse aspects of high-valent iron, see: a) A. Ghosh, *J. Inorg. Biochem.* **2006**, 100, 419; b) J. Hohenberger, K. Ray, K. Meyer, *Nature Comm.* **2012**, 3, 720.
- [8] J. K. M. Sanders, N. Bampos, Z. Clyde-Watson, S. L. Darling, J. C. Hawley, H.-J. Kim, C. C. Mak, S. J. Webb, *Axial Coordination Chemistry of Metalloporphyrins. In The Porphyrin Handbook*; Ed. K. M. Kadish, K. M. Smith, R. Guilard, Academic Press, **2000**, vol 3, 1–48.
- [9] a) Ghosh, A. *Chem. Rev.* **2017**, 117, 3798; b) S. Nardis, F. Mandoj, M. Stefanelli, R. Paolesse, *Coord. Chem. Rev.* **2019**, 388, 360.
- [10] A. B. Alemayehu, H. Vazquez-Lima, K. J. Gagnon, A. Ghosh, *Inorg. Chem.* **2017**, 56, 5285.
- [11] A. B. Alemayehu, K. J. Gagnon, J. Turner, A. Ghosh, *Angew. Chem. Int. Ed.* **2014**, 53, 14411.
- [12] A. B. Alemayehu, H. Vazquez-Lima, L. J. McCormick, A. Ghosh, *Chem. Eur. J.* **2016**, 22, 6914. *Chem. Commun.* **2017**, 53, 5830.
- [13] A. B. Alemayehu, H. Vazquez-Lima, K. J. Gagnon, A. Ghosh, *Chem. Eur. J.* **2016**, 22, 6914.
- [14] a) W. Bronger, W. L. à Brassard, P. Müller, B. Lebeck, T. Schultz, *Z. Anorg. Allg. Chem.* **1999**, 625, 1143; See also: b) S. Takagi, Y. Iijima, T. Sato, H. Saitoh, K. Ikeda, T. Otomo, K. Miwa, T. Ikeshoji, S.-I. Orimo, *Sci. Rep.* **2017**, 7, 44253.
- [15] R. F. Einrem, K. J. Gagnon, A. B. Alemayehu, A. Ghosh, *Chem. Eur. J.* **2016**, 22, 517.
- [16] a) J. H. Palmer, A. C. Durrell, Z. Gross, J. R. Winkler, H. B. Gray, *J. Am. Chem. Soc.* **2008**, 130, 7786; b) J. H. Palmer, A. Mahammed, K. M. Lancaster, Z. Gross, H. B. Gray, *Inorg. Chem.* **2009**, 48, 9308.
- [17] J. H. Palmer, K. M. Lancaster, *Inorg. Chem.* **2012**, 51, 12473.
- [18] For a review, see: D. B. Papkovsky, T. C. O'Riordan, *J. Fluoresc.* **2005**, 15, 569.
- [19] For selected studies from our laboratory, see: a) S. M. Borisov, A. B. Alemayehu, A. Ghosh, *J. Mater. Chem. C* **2016**, 4, 5822; b) A. B. Alemayehu, N. U. Day, T. Mani, A. B. Rudine, K. E. Thomas, O. A. Gederaas, S. A. Vinogradov, C. C. Wamser, A. Ghosh, *ACS Appl. Mater. Interfaces* **2016**, 8, 18935; c) A. B. Alemayehu, L. J. McCormick, K. J. Gagnon, S. M. Borisov, A. Ghosh, *ACS Omega* **2018**, 3, 9360; d) S. M. Borisov, R. F. Einrem, A. B. Alemayehu, A. Ghosh, *Photochem. Photobiol. Sci.* **2019**, 18, 1166.
- [20] a) M. A. Muckey, L. F. Szczepura, G. M. Ferrence, T. D. Lash, *Inorg. Chem.* **2002**, 41, 4840; b) T. D. Lash, D. A. Colby, L. F. Szczepura, *Inorg. Chem.* **2004**, 43, 5258; c) V. A. K. Adiraju, G. M. Ferrence, T. D. Lash, *Dalton Trans.* **2016**, 45, 13691.
- [21] a) M. Pawlicki, L. Latos-Grażyński, *Carbaporphyrinoids - Synthesis and Coordination Properties. In Handbook of Porphyrin Science: with Applications to Chemistry, Physics, Materials Science, Engineering, Biology and Medicine. K. M. Kadish, K. M. Smith, R. Guilard, Eds. World Scientific, Singapore*, **2010**, Vol. 2, Ch. 8, pp 104–192; b) D. Lash, *Chem. Rev.* **2017**, 117, 2313.
- [22] a) P. Pyykkö, S. Riedel, M. Patzschke, *Chem. Eur. J.* **2005**, 11, 3511; b) P. Pyykkö, M. Atsumi, *Chem. Eur. J.* **2009**, 15, 186; c) P. Pyykkö, M. Atsumi, *Chem. Eur. J.* **2009**, 15, 12770.
- [23] J. Stephens, F. J. Devlin, C. F. Chabalowski, M. J. Frisch, *J. Phys. Chem.* **1994**, 98, 11623.
- [24] G. te Velde, F. M. Bickelhaupt, S. J. A. van Gisbergen, C. Fonseca Guerra, E. J. Baerends, J. G. Snijders, T. Ziegler, *J. Comput. Chem.* **2001**, 22, 931.
- [25] For recent studies of carbaporphyrinoid aromaticity in our laboratory, see: a) A. Ghosh, S. Larsen, J. Conradie, C. Foroutan-Nejad, *Org. Biomol. Chem.* **2018**, 16, 7964; b) S. Larsen, L. J. McCormick-McPherson, S. J. Teat, A. Ghosh *ACS Omega* **2019**, 4, 6737.
- [26] L. Krause, R. Herbst-Irmer, G. M. Sheldrick, D. Stalke, *J. Appl. Crystallogr.* **2015**, 48, 3.
- [27] G. M. Sheldrick, *Acta Crystallogr.* **2015**, A71, 3.
- [28] G. M. Sheldrick, *Acta Crystallogr.* **2015**, C71, 3.

Manuscript received: September 5, 2019
Revised manuscript received: September 25, 2019